J. Fluid Mech. (1972), *vol.* 56, *part* 2, *pp.* 277–286
Printed in Great Britain

Waves in a gas in solid-body rotation

By J. B. MORTON AND E. J. SHAUGHNESSY
Department of Aerospace Engineering and Engineering Physics,
University of Virginia, Charlottesville

(Received 9 December 1971 and in revised form 20 July 1972)

The axial and transverse wave motions of an inviscid perfect gas in isothermal solid-body rotation in a cylinder are investigated. Solutions of the resulting eigenvalue problem are shown to correspond to two types of waves. The acoustic waves are the rotational counterparts of the well-known Rayleigh solutions for a gas at rest in a cylinder. The rotational waves, whose amplitudes and frequencies go to zero in the non-rotating limit, exhibit phase speeds both larger and smaller than the speed of sound. The effect of rotation on the frequency and structure of these waves is discussed.

1. Introduction

Wave motions in incompressible rotating fluids have been extensively studied (Greenspan 1968; Lamb 1932) because of their application to problems of geophysical origin. To date, however, there have been relatively few investigations of waves in rotating fluids in which compressibility has been considered. The purpose of this paper is to consider waves in a flow of practical importance: isothermal solid-body rotation in a cylinder.

Many investigations of wave motions in gases have explored the effect of container shape (Lamb 1932; Rayleigh 1896). In particular, Rayleigh's (1896, p. 300) study of the waves in a uniform gas in a cylinder discussed the zero-rotation solution for the present problem. In the same way, Maslen & Moore's (1956) viscous analysis of the transverse waves in a gas at rest in a cylinder formulated the basis for a viscous treatment of the rotating problem.

A more recent effort by Fraenkel (1959) discussed the propagation of a cylindrical sound pulse into an infinite mass of gas initially in isothermal solid-body rotation and noted the oscillatory influence of the Coriolis force. Salant (1968) considered the symmetric standing waves in an isothermal gas in a rotating cylinder while Sozou (1969*a*) discussed the same waves for a gas in isentropic solid-body rotation. Later Sozou (1969*a*) investigated the transverse wave motions for the same initial state and found acoustic solutions.† Finally, Sozou & Swithen bank (1969) examined the transverse wave motions in a Rankine vortex. This time, in addition to acoustic waves, they found slow waves.‡

In the present paper the axial and transverse wave motions of an inviscid perfect gas in isothermal solid-body rotation are investigated for a range of rotation

† These reduce to the Rayleigh solutions in the zero-rotation limit.
‡ Their terminology.

rates and wavenumbers. Two types of waves are discussed: acoustic waves, which are the rotational extension of the Rayleigh solutions, and rotational waves, whose amplitude and frequency go to zero in the non-rotating limit. Spiralling waves, which have both axial and transverse components, are not considered here but can be handled in the same manner.

2. Theory

2.1. *The steady-state motion*

Let (r, θ, z) be cylindrical polar co-ordinates fixed in space and (U, V, W) the corresponding components of velocity. The z axis lies along the axis of symmetry of the infinitely long right circular cylinder containing the gas. Since the velocity components of a gas in solid-body rotation about the z axis at angular velocity Ω are given by

$$U = 0, \quad V = r\Omega, \quad W = 0, \tag{2.1}$$

the pressure distribution is governed by the hydrostatic equation

$$d\hat{p}/dr = \hat{\rho} r \Omega^2, \tag{2.2}$$

where $\hat{p}$ is the pressure and $\hat{\rho}$ the density.

For a perfect gas at uniform temperature T the pressure distribution in the cylinder is

$$\hat{p} = \hat{p}_0 \exp\{-\tfrac{1}{2}\gamma A^2 [1-(r/r_0)^2]\}, \tag{2.3}$$

where r_0 is the radius of the cylinder, γ the ratio of specific heats, $c_0 = (\gamma RT)^{\frac{1}{2}}$ the sound speed, $A = r_0 \Omega / c_0$ the peripheral Mach number and $\hat{p}_0$ the pressure at the cylinder wall.

2.2. *Disturbance equation*

Let (u', v', w') be small† perturbations of the steady-state velocity components (U, V, W) with p' and ρ' the corresponding perturbations of the steady-state pressure $\hat{p}$ and density $\hat{\rho}$. Neglecting viscous and thermal conduction effects on the wave motions, and dropping all second-order perturbation terms, the continuity, momentum and energy equations become

$$\frac{\partial \rho'}{\partial t} + \frac{1}{r}\frac{\partial}{\partial r}(r\hat{\rho}u') + \frac{1}{r}\frac{\partial}{\partial \theta}(\hat{\rho}v' + \rho' r\Omega) + \frac{\partial}{\partial z}(\hat{\rho}w') = 0, \tag{2.4}$$

$$\hat{\rho}\left[\frac{\partial u'}{\partial t} + \Omega\frac{\partial u'}{\partial \theta} - 2\Omega v'\right] - \rho' r\Omega^2 = -\frac{\partial p'}{\partial r}, \tag{2.5}$$

$$\hat{\rho}\left[\frac{\partial v'}{\partial t} + \Omega\frac{\partial v'}{\partial \theta} + 2\Omega u'\right] = -\frac{1}{r}\frac{\partial p'}{\partial \theta}, \tag{2.6}$$

$$\hat{\rho}\left[\frac{\partial w'}{\partial t} + \Omega\frac{\partial w'}{\partial \theta}\right] = -\frac{\partial p'}{\partial z}, \tag{2.7}$$

$$\left[\frac{\partial p'}{\partial t} + \Omega\frac{\partial p'}{\partial \theta}\right] - c_0^2\left[\frac{\partial \rho'}{\partial t} + \Omega\frac{\partial \rho'}{\partial \theta}\right] = u'(\gamma-1)\frac{d\hat{p}}{dr}. \tag{2.8}$$

By assuming periodic disturbances of the form

$$(u', v', w', p', \rho') = (u^*(r), v^*(r), w^*(r), p^*(r), \rho^*(r)) \exp[i(n\theta + kz - \sigma t)], \tag{2.9}$$

† Small compared with $r_0\Omega$.

where n is an integer, and non-dimensionalizing according to

$$\left.\begin{aligned} p = p^*/p_0, \quad \rho = \rho^*\frac{c_0^2}{p_0}, \quad \tilde{\rho} = \hat{\rho}\frac{c_0^2}{p_0}, \quad (u,v,w) = (u^*,v^*,w^*)/c_0, \\ \lambda = \frac{-\sigma+n\Omega}{c_0}r_0, \quad A = \frac{\Omega r_0}{c_0}, \quad x = r/r_0, \quad \alpha = r_0 k, \end{aligned}\right\} \tag{2.10}$$

equations (2.4)–(2.8) can be reduced with the substitution $q = xu$ to the single equation

$$\frac{d^2q}{dx^2}-\frac{1}{x}\frac{dq}{dx}\left[1-\gamma A^2x^2+\frac{2n^2}{(\lambda^2-\alpha^2)x^2-n^2}\right]-q\left[\frac{2n^2A^2}{(\lambda^2-\alpha^2)x^2-n^2}-\frac{4nA(\lambda^2-\alpha^2)}{\lambda[(\lambda^2-\alpha^2)x^2-n^2]}\right.$$
$$\left.-\frac{(4-2\gamma)A^3n}{\lambda}-\frac{A^4(\gamma-1)}{\lambda^2}(\alpha^2x^2+n^2)-(\lambda^2-\alpha^2)+\frac{n^2}{x^2}+\frac{4(\lambda^2-\alpha^2)A^2}{\lambda^2}\right]=0. \tag{2.11}$$

Since the radial mass flow must be zero at the axis and at the cylinder wall, the boundary conditions for (2.11) are $q(0) = q(1) = 0$. The original system is thus reduced to an eigenvalue problem for a second-order ordinary differential equation. Given a pair of wavenumbers (n, α), each of the infinite number of eigenfunction–eigenvalue pairs (q, λ) corresponds to a possible wave mode for that wavenumber pair. The wave frequency σ is related to the eigenvalue λ through relation (2.10). Similarly the eigenfunction q is related to the following physical quantities of interest:

$$p = \frac{i\lambda\tilde{\rho}}{(\lambda^2-\alpha^2)x^2-n^2}\left\{A^2x^2q-\frac{2Anq}{\lambda}+x\frac{dq}{dx}\right\}, \tag{2.12}$$

$$w = -\frac{i\alpha}{(\lambda^2-\alpha^2)x^2-n^2}\left\{A^2x^2q-\frac{2Anq}{\lambda}+x\frac{dq}{dx}\right\}, \tag{2.13}$$

$$v = -\frac{in}{x[(\lambda^2-\alpha^2)x^2-n^2]}\left\{A^2x^2q-\frac{2An}{\lambda}q+x\frac{dq}{dx}\right\}+\frac{2Aq}{\lambda x}i, \tag{2.14}$$

$$\rho = \frac{i(\gamma-1)qA^2\tilde{\rho}}{\lambda}+\frac{i\lambda\tilde{\rho}}{(\lambda^2-\alpha^2)x^2-n^2}\left\{A^2x^2q-\frac{2An}{\lambda}q+x\frac{dq}{dx}\right\}. \tag{2.15}$$

There are two singularities in (2.11). The x^{-1} term reflects the requirement of conservation of mass in the cylindrical geometry while the singularity at $x = n/(\lambda^2-\alpha^2)^{\frac{1}{2}}$ corresponds to the point in the flow where the phase speed of the wave in the direction of propagation equals the undisturbed sound speed.

2.3. *Numerical computation*

The numerical method used in this paper is based on a shooting method of finding eigenvalues. A power-series solution near the origin, extended by a combined Runge–Kutta and Adams–Moulton method, was used to integrate (2.11) after an initial guess for the eigenvalue. Then a simple root-finder technique was used to find the eigenvalue to an accuracy of at least four significant digits. The singularity at $x = n/(\lambda^2-\alpha^2)^{\frac{1}{2}}$ caused no difficulty as long as its location did not coincide with any mesh point used in the integration. All calculations in this paper are for $\gamma = 1{\cdot}4$.

2.4. *Non-rotating solutions*

Rayleigh (1896, p. 300) solved (2.1) for the non-rotating ($A = 0$) case in terms of the derivatives of Bessel functions of order n. The eigenfunction–eigenvalue pair is

$$q(x) = a_0 x J_n'[(\lambda^2-\alpha^2)^{\frac{1}{2}}x], \quad \lambda^2 = \alpha^2 + (j'_{m,n})^2, \tag{2.16}$$

where J_n' is the derivative of the Bessel function of order n and $j'_{m,n}$ is the mth zero of this function. When $n = 0$, the eigenvalue $\lambda = \alpha$ is also allowable. Extensive tables of these functions appear in Abramowitz & Stegun (1968, p. 411).

3. Axial waves

When $n = 0$ the solutions of (2.11) describe axisymmetric wave motions which propagate parallel to the cylinder axis. These axial waves are characterized by the phase speed

$$V_l = \sigma/k. \tag{3.1}$$

In the non-rotating case, the Rayleigh solution for the frequency yields the phase speed distribution

$$V_l^2/c_0^2 = 1 + (j'_{m,0})^2/\alpha^2, \tag{3.2}$$

hence these disturbances all travel faster than the undisturbed sound speed. When $\lambda = \alpha$, $V_l = c_0$ so the wave is a plane sound wave. In the rotating case, $\lambda = \alpha$ corresponds to a sound wave with a radial pressure distribution

$$p \sim \exp[r^2\Omega^2/c_0^2].$$

For axial waves in the rotating gas, the disturbance equation is

$$\frac{d^2q}{dx^2} - \frac{1}{x}\frac{dq}{dx}\{1-\gamma A^2x^2\} - q\left\{\frac{(4A^2-\lambda^2)(\lambda^2-\alpha^2)}{\lambda^2} - A^4\frac{\gamma-1}{\lambda^2}\alpha^2x^2\right\} = 0, \tag{3.3}$$

subject to the same boundary conditions as before.

Solutions to (3.3) can be given in terms of the confluent hypergeometric function ${}_1F_1$,† with frequencies determined by the zeros of this function. Unfortunately these zeros are not well tabulated, necessitating numerical methods in general. However, an approximate method based on the transformation

$$q(x) = f(x)\,x\exp[\tfrac{1}{4}\gamma A^2x^2] \tag{3.4}$$

has proved useful for determining frequencies. For small rotation rates ($A \ll 1$) the transformed equation may be simplified to Bessel's equation. The resulting frequency relation is

$$\lambda^2 = [(j_{m,1})^2+\alpha^2+4A^2]\left\{\frac{1}{2} \pm \frac{1}{2}\left(1-\frac{16\alpha^2A^2}{[(j_{m,1})^2+\alpha^2+4A^2]^2}\right)^{\frac{1}{2}}\right\}. \tag{3.5‡}$$

† The notation follows Slater (1960).

‡ $j_{m,1}$ is the mth zero of the Bessel function of order 1.

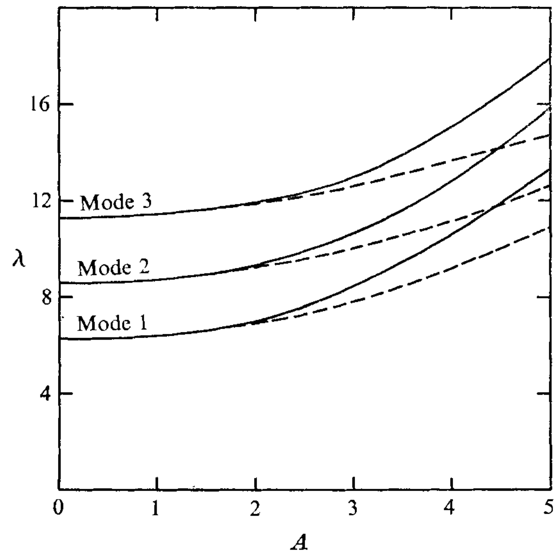

FIGURE 1. Axial wave frequencies ($n = 0$, $\alpha = 5$) for acoustic waves: three modes. – –, approximate result [equation (3.5)].

The class of axial solutions contains two distinct types of waves depending on the sign of the term in curly brackets in (3.5). It is easily verified that acoustic wave frequencies, corresponding to the positive sign, reduce to the Rayleigh frequencies as $A \to 0$. On the other hand, the frequencies (and amplitudes) of rotational waves, corresponding to the negative sign, tend to zero in the same limit. This conclusion is confirmed by the numerical results.

3.1. *Acoustic waves*

The effect of rotation rate on the frequencies of the first three modes of a typical acoustic wave is shown in figure 1. The results of the approximate relation (3.5) are also included, and it can be seen that the agreement is quite good at moderate rotation rates. For all wavenumbers the frequency of a wave increases with increasing rotation rate, with the lowest modes (smallest frequencies) being proportionately more affected. The slope of the frequency *vs.* rotation rate curve at a given rotation rate decreases with increasing wavenumber. Higher frequency acoustic waves are influenced less by the rotation than lower frequency waves.

The normalized radial pressure distribution in an acoustic wave is shown in figure 2 (*a*) as a function of distance from the axis in units of radii. The rotation rate is $A = 3$. In figure 2 (*b*) the pressure distribution in the first mode of the same wave is shown for different rotation rates. The different appearance of the $A = 3$ wave is due to normalization at $x = 1$ rather than at $x = 0$.

3.2. *Rotational waves*

In contrast to acoustic waves, the mode frequencies of rotational waves are restricted to a finite band located between the mode 1 frequency and zero. This can be seen in figure 3, which gives the frequencies of a typical rotational wave.

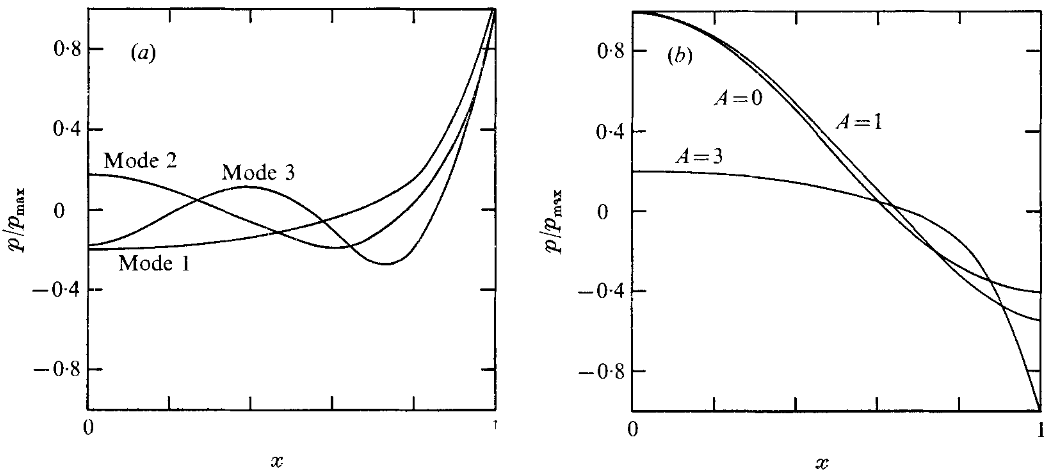

FIGURE 2. Axial wave pressure distribution ($n = 0$, $\alpha = 5$) for acoustic waves. (a) $A = 3$, three modes. (b) First mode, $A = 0$, 1 and 3.

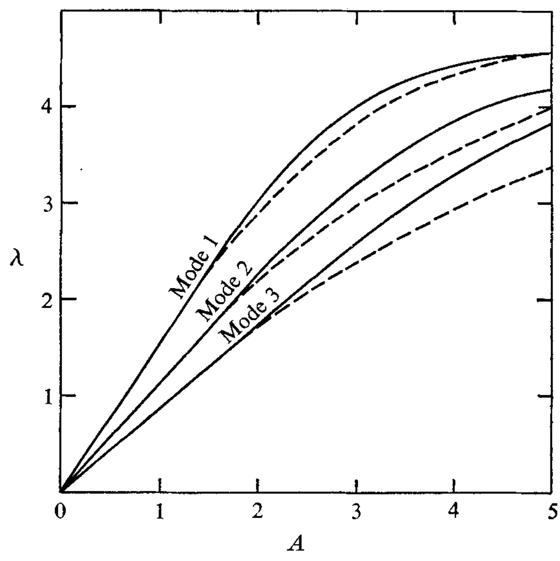

FIGURE 3. Axial wave frequencies ($n = 0$, $\alpha = 5$) for rotational waves: three modes. ——, approximate result [equation (3.5)].

Since $\alpha = 5$ in this case, the line $\lambda = 5$ gives the frequency of a sound wave, and it appears that regardless of the value of the rotation rate rotational waves propagate at speeds less than the speed of sound. The values determined by the approximate result (3.5) are again seen to be in good agreement with the numerical results.

The pressure distribution in a rotational wave is remarkably similar to that of an acoustic wave as seen earlier in figure 2 (b). The same is true for the change in pressure distribution with rotation rate.

4. Transverse waves

When $\alpha = 0$ the solutions of (2.11) describe motions which occur in planes normal to the cylinder axis. These transverse waves are characterized by the phase angular velocity σ/n and peripheral phase speed

$$V_\theta = \sigma r_0/n. \tag{4.1}$$

Since an observer fixed in the rotating cylinder sees a peripheral phase speed $r_0(\sigma/n - \Omega)$, the quantity

$$\frac{\lambda}{n} = -\frac{r_0}{c_0}\left(\frac{\sigma}{n} - \Omega\right)$$

is the negative of the non-dimensional phase speed seen by this observer.

In the non-rotating case, Rayleigh's solution for the frequency

$$\lambda = \pm j'_{m,n} \tag{4.2}$$

indicates there are two identical waves, one travelling in each direction around the cylinder. In the rotating case, the situation is more complex. For a given wavenumber and mode number, there are two waves of each type (acoustic and rotational), which travel in opposite directions around the cylinder. In general, the frequency and wave structure of the pair differ.

The equation governing transverse waves is

$$\frac{d^2q}{dx^2} - \frac{1}{x}\frac{dq}{dx}\left\{1 - \gamma A^2x^2 + \frac{2n^2}{\lambda^2x^2 - n^2}\right\} + q\left\{-\frac{2n^2A^2}{\lambda^2x^2 - n^2} + \frac{4nA\lambda}{\lambda^2x^2 - n^2} + \frac{(4-2\gamma)A^3n}{\lambda} + \frac{A^4(\gamma-1)n^2}{\lambda^2} + \frac{(\lambda^2x^2 - n^2)}{x^2} - 4A^2\right\} = 0. \tag{4.3}$$

Because the equation is unaffected by the substitution $(-\lambda, A) \to (\lambda, -A)$ it proves convenient to determine negative frequencies as the positive ones which correspond to a negative rotation rate A. Thus, in the figures, λ values on the left halves correspond to negative frequencies and therefore to waves which travel in the direction of fluid rotation relative to the cylinder.

For small rotation rates, the following analysis provides a useful method of determining the rotational wave frequencies. Writing q and λ as power series in A,

$$\left.\begin{aligned} q(x, A, \lambda) &= Aq_0(x, j_{m,n}) + A^2q_1(x, j_{m,n}) + \ldots, \\ \lambda &= \frac{n(\gamma-1)^{\frac{1}{2}}}{j_{m,n}} A^2\{1 + \epsilon_1 A + \epsilon_2 A^2 + \ldots\}, \end{aligned}\right\} \tag{4.4}$$

and substituting into (4.3) yields after some analysis

$$\left.\begin{aligned} &\epsilon_1 = \frac{2-\gamma}{j_{m,n}(\gamma-1)^{\frac{1}{2}}}, \quad \epsilon_2 = \frac{6-5\gamma}{2j_{m,n}^2(\gamma-1)}, \quad \epsilon_3 = \frac{\gamma^2-2\gamma-2}{j_{m,n}^3(\gamma-1)^{\frac{1}{2}}}, \\ &\epsilon_4 = -\frac{(2-\gamma)^4}{8j_{m\,n}^4(\gamma-1)^2} - \frac{3}{4}\frac{2+\gamma}{j_{m,n}^4(\gamma-1)}(2-\gamma)^2 + 3\frac{(2+\gamma)^2}{8j_{m,n}^4} \\ &\qquad - \frac{(n^2-2)(\gamma-1)}{2j_{m,n}^4} - \frac{6(2-\gamma)}{j_{m,n}^4} - \frac{\gamma^2}{24j_{m,n}^2}. \end{aligned}\right\} \tag{4.5}$$

A	Series	Numerical
0·5	0·0072283	0·0072283
1	0·034084	0·034090
2	0·171967	0·17343
3	0·392683	0·43108

TABLE 1. Frequencies for $n = 1$, third mode, transverse wave

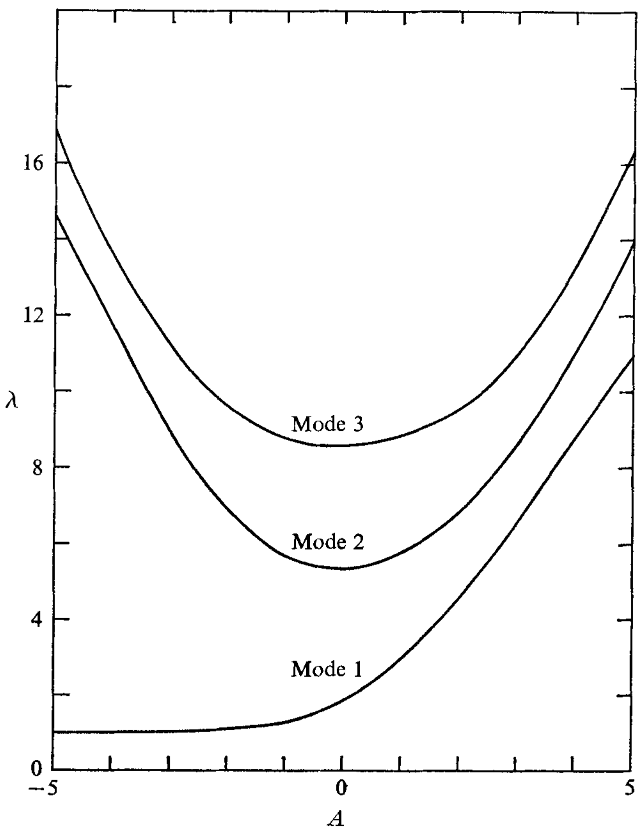

FIGURE 4. Transverse wave frequencies ($n = 1$, $\alpha = 0$) for acoustic waves: three modes.

Table 1 contains a comparison between the values of λ obtained by this method and the numerical values for a typical rotational wave. In general, the larger $j_{m,n}$, the faster the series converges provided that A is not too large.

A similar perturbation analysis of the equations derived by Sozou (1969*b*) for the case of isentropic solid-body rotation fails to yield solutions of the rotational type.

4.1. *Acoustic waves*

The effect of rotation rate on the frequencies of the first three modes of a typical acoustic wave is shown in figure 4. Apart from that of the first mode wave travelling in the direction of fluid rotation, all mode frequencies increase with increasing

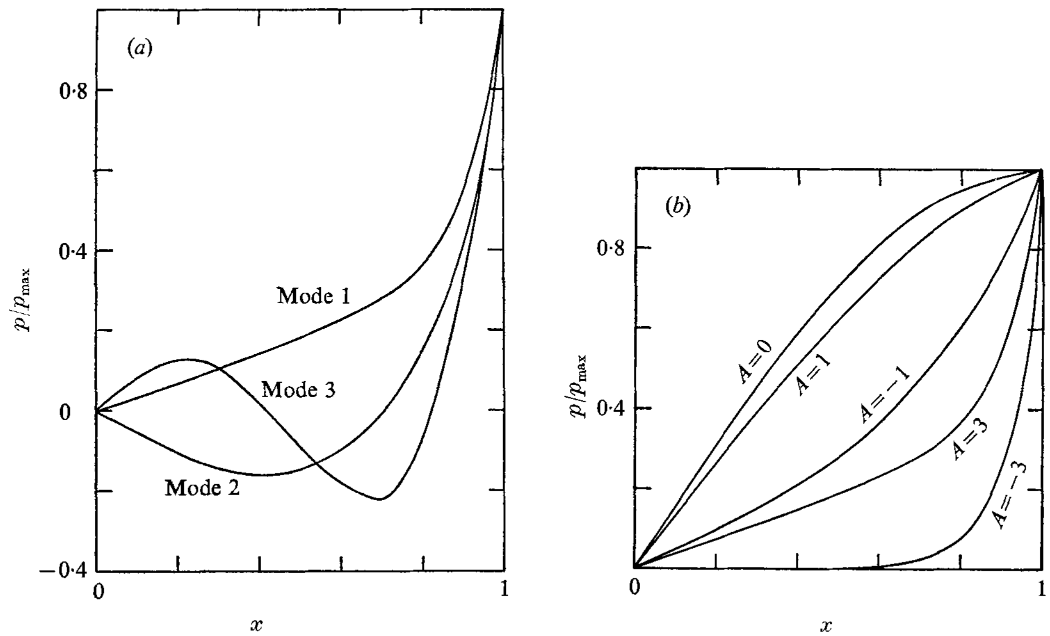

FIGURE 5. Transverse wave pressure distribution ($n = 1$, $\alpha = 0$) for acoustic waves. (a) $A = 3$, three modes. (b) First mode, $A = 0$, ± 1, and ± 3.

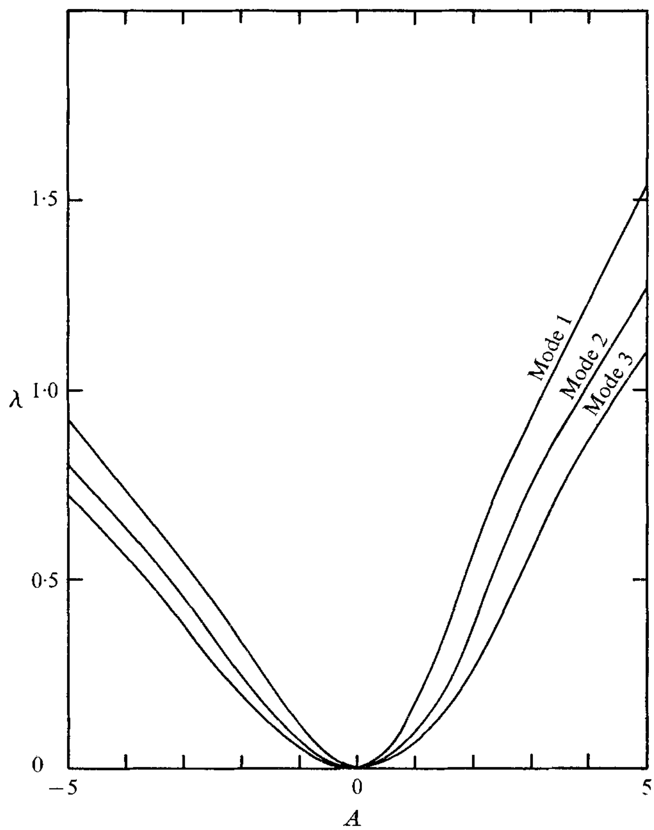

FIGURE 6. Transverse wave frequencies ($n = 1$, $\alpha = 0$) for rotational waves: three modes.

rotation rate. The frequency of the first mode travelling in the direction of the rotation tends towards the value $\lambda = n$ with increasing rotation rate. This corresponds to a peripheral phase speed relative to the cylinder equal to the undisturbed sound speed. All first-mode acoustic waves exhibit this behaviour.

The normalized radial pressure distribution in an acoustic wave is shown in figure 5(*a*) for three modes. In figure 5(*b*) the pressure distribution in the first mode of the same wave is shown for different rotation rates. Recall that negative A values correspond to waves travelling in the direction of fluid rotation.

4.2. *Rotational waves*

Like axial waves, transverse rotational waves have their frequencies restricted to a band between the mode 1 frequency curve and zero. This can be seen in figure 6, which gives the frequencies of a typical rotational wave. Unlike axial rotational waves, however, these waves may propagate with peripheral phase speeds which are faster than the speed of sound. In figure 6, frequencies above the line $\lambda = 1{\cdot}0$ correspond to just such waves.

The pressure distributions in rotational waves are again very similar to those of acoustics waves shown in figures 5(*a*) and (*b*).

REFERENCES

ABRAMOWITZ, M. & STEGUN, I. A. 1968 *Handbook of Mathematical Functions.* Washington: U.S. Government Printing Office.

FRAENKEL, L. E. 1959 *J. Fluid Mech.* **5**, 637–649.

GREENSPAN, H. P. 1968 *The Theory of Rotating Fluids.* Cambridge University Press.

LAMB, H. 1932 *Hydrodynamics*, 6th edn. Dover.

MASLEN, S. H. & MOORE, F. K. 1956 *J. Aero Sci.* **23**, 583.

RAYLEIGH, LORD 1896 *The Theory of Sound*, 2nd edn. Dover.

SALANT, R. F. 1968 *J. Acoust. Soc. Am.* **43**, 1302–1305.

SLATER, L. J. 1960 *Confluent Hypergeometric Functions.* Cambridge University Press.

SOZOU, C. 1969*a* *J. Acoust. Soc. Am.* **46**, 814–818.

SOZOU, C. 1969*b* *J. Fluid Mech.* **36**, 605–612.

SOZOU, C. & SWITHENBANK, J. 1969 *J. Fluid Mech.* **38**, 657–671.